

# LC-MS/MS based untargeted lipidomics uncovers lipid signatures of the human placenta from intrahepatic cholestasis of pregnancy

Liling Xiong<sup>1</sup>, Mi Tang<sup>1</sup>, Hong Liu<sup>1</sup>, Jianghui Cai<sup>1</sup>, Ying Jin<sup>1</sup>, Xiu Yang<sup>1</sup>, Cheng Huang<sup>1</sup>, Shasha Xing<sup>1</sup>, and Xiao Yang<sup>1</sup>

<sup>1</sup>University of Electronic Science and Technology of China School of Electronic Science and Engineering

July 14, 2023

## Abstract

**Objective:** To explore the characteristic lipid signature in placentas collected from normal pregnancies and those with mild and severe intrahepatic cholestasis of pregnancy (ICP). This research aims to clarify the pathogenesis and identify lipid biomarker for ICP through LC-MS/MS based lipidomic analysis. **Design:** Cross-sectional study, including normal pregnancy women and women with mild and severe ICP. **Setting:** Chengdu Women's and Children's Center Hospital. **Population:** Placenta samples collected from 30 normal pregnancy women and 30 mild and severe ICP women respectively. Women with normal pregnancy and ICP were recruit from April 2021 to July 2022 in Chengdu, China. **Main outcome measures:** Differentially expressed lipids. **Results:** Forty-four lipids were differentially expressed both in mild and severe ICP placenta. The pathway analysis revealed these lipids are mainly enriched in glycerophospholipid metabolism and autophagy pathway. Weighted correlation network analysis (WGCNA) identified the correlation network module of lipids highly related to ICP. Using multiple logistic regression analysis, we identified three and four combined metabolites that had an area under receiver operating characteristic curves (AUC) [?] 0.90. **Conclusion:** Our results systematically revealed the lipid signature in mild and severe ICP placenta. The results may provide new insight into the treatment and early prediction of ICP.

## LC-MS/MS based untargeted lipidomics uncovers lipid signatures of the human placenta from intrahepatic cholestasis of pregnancy

Liling Xiong<sup>1#</sup>, Mi Tang<sup>3#</sup>, Hong Liu<sup>1</sup>, Jianghui Cai<sup>4</sup>, Ying Jin<sup>1</sup>, Xiu Yang<sup>1</sup>, Cheng Huang<sup>2</sup>, Shasha Xing<sup>3\*</sup>, Xiao Yang<sup>1\*</sup>

<sup>1</sup>, *Obstetricsdepartment*, Chengdu Women's and Children's Center Hospital, School of Medicine, University of Electronic Science and Technology of China, Chengdu, 611731, China

<sup>2</sup>, *Clinicallab*, Chengdu Women's and Children's Center Hospital, School of Medicine, University of Electronic Science and Technology of China, Chengdu, 611731, China

<sup>3</sup>, GCP institution, Chengdu Women's and Children's Center Hospital, School of Medicine, University of Electronic Science and Technology of China, Chengdu, 611731, China

<sup>4</sup>, Department of Pharmacy, Chengdu Women's and Children's Center Hospital, School of Medicine, University of Electronic Science and Technology of China, Chengdu, 611731, China

# These authors contributed equally to this work

\* These authors contributed equally to this work

Send Correspondence and Reprint Request to:

Xiao Yang, M.D and Ph.D.

Tel: (8628) 6186-6124

Fax: (8628)6186-6124

E-mail: [wchgcptg@163.com](mailto:wchgcptg@163.com)

Address: Chengdu Women's and Children's Center Hospital, 1617 Riyue Avenue, Qingyang district, Chengdu City, Sichuan Province, China.

### Abstract:

**Objective:** To explore the characteristic lipid signature in placentas collected from normal pregnancies and those with mild and severe intrahepatic cholestasis of pregnancy (ICP). This research aims to clarify the pathogenesis and identify lipid biomarker for ICP through LC-MS/MS based lipidomic analysis.

**Design:** Cross-sectional study, including normal pregnancy women and women with mild and severe ICP.

**Setting:** Chengdu Women's and Children's Center Hospital.

**Population:** Placenta samples collected from 30 normal pregnancy women and 30 mild and severe ICP women respectively. Women with normal pregnancy and ICP were recruit from April 2021 to July 2022 in Chengdu, China.

**Main outcome measures:** Differentially expressed lipids.

**Results:** Forty-four lipids were differentially expressed both in mild and severe ICP placenta. The pathway analysis revealed these lipids are mainly enriched in glycerophospholipid metabolism and autophagy pathway. Weighted correlation network analysis (WGCNA) identified the correlation network module of lipids highly related to ICP. Using multiple logistic regression analysis, we identified three and four combined metabolites that had an area under receiver operating characteristic curves (AUC) [?] 0.90.

**Conclusion:** Our results systematically revealed the lipid signature in mild and severe ICP placenta. The results may provide new insight into the treatment and early prediction of ICP.

**Keywords:** Intrahepatic cholestasis of pregnancy, lipidomics, phosphatidylethanolamine, sphingolipids, autophagy

### Introduction

Intrahepatic cholestasis of pregnancy (ICP) is the most common pregnancy-specific liver disease that usually occurs in the second or third trimester of pregnancy. Its clinical manifestations are mild to severe persistent pruritus, abnormal liver function, and elevated total bile acid (TBA) levels<sup>1, 2</sup>. Although ICP is rarely harmful to the mother, it poses a significant risk to the fetus of perinatal complications such as preterm birth, meconium-stained amniotic fluid, neonatal depression, respiratory distress syndrome and stillbirth<sup>3</sup>. The incidence of ICP varies geographically and demographically from 0.1 to 15.6%<sup>4</sup>. Nowadays, there is no effective treatment for ICP, administration of ursodeoxycholic acid (UDCA) is one of the choices. UDCA was proven to relieve pruritus and decrease bile acid levels, though it is of unproven benefit in preventing adverse effects on the fetus<sup>5, 6</sup>. At present, there is a lack of consensus on the diagnostic criteria for ICP. Most guidelines agree on the requirement of pruritus and abnormal liver enzymes, the most sensitive biochemical index used in the diagnostics of ICP is the level of total bile acids. The European Association for the Study of the Liver (EASL) and the Society for Maternal-Fetal Medicine (SMFM) propose persistent pruritus that resolves with delivery and bile acid concentrations > 10 $\mu$ mol/L for diagnosis<sup>7</sup>. Many prospective studies revealed that TBA level [?] 40 $\mu$ mol/L was associated with an increased risk of adverse neonatal outcomes in ICP<sup>8, 9</sup>. However, evidence proved TBA levels alone are not a sufficiently sensitive and specific marker for this disease. According to a retrospective study conducted by Kondrackiene et al, concentrations of cholic acid (CA), chenodeoxycholic acid (CDCA), and the CA/CDCA ratio are better markers<sup>10, 11</sup>. Accordingly, there is growing interest in identifying new markers with diagnostic and prognostic value in ICP.

The pathogenesis of ICP remains unknown, there are several theories about the causes of ICP, including the estrogen–bile acid axis, placental hypoxia, lipid metabolism disorders and trophoblast autophagy<sup>12-14</sup>. As a subcategory of metabolic profiling, lipidomics can efficiently analyze lipid molecule changes in various pathophysiological processes<sup>15</sup>. More and more evidence proved that abnormal lipid metabolism is closely related to various pregnancy-related diseases such as preeclampsia, gestational diabetes mellitus, and preterm birth<sup>16-18</sup>. Since ICP is closely related to bile acid metabolism, metabolomic technology has become an effective method for finding diagnostic markers in serum, urine, and even hair samples of ICP patients in recent years. Metabolomic signatures from serum and urine can be used as biomarkers for the diagnosis of ICP<sup>19, 20</sup>. In recent years, more and more studies believe that lipid metabolism is closely related to the occurrence and development of ICP, the dysregulation of bile acid in serum and placenta will lead to abnormal lipid metabolism to a large extent, and then increase the risk of ICP<sup>21</sup>. High triglyceride concentrations in the second and third trimesters have been reported to be associated with an increased risk of ICP, possibly due to reduced activity of bile acid receptors FXR and TGR5<sup>22</sup>. A more recent untargeted lipidomics study revealed the abnormal lipid profiles of plasma collected from ICP patients and suggests that sphingolipid metabolism dysregulation may be associated with the development of ICP<sup>23</sup>. Therefore, using lipid metabolites as clues may help us to further explore the molecular mechanisms underlying the occurrence of intrahepatic cholestasis of pregnancy.

In this study, LC-MS/MS based untargeted lipidomics was applied to investigate lipidomics profiling of placentas from women with normal pregnancies and those with mild or severe ICP. And we also uncovered a group of lipids with high accuracy in identifying and diagnosing ICP. Our findings may provide new insights into the pathogenesis and prediction of ICP.

## Materials and methods

### Clinical specimen collection and preparation

The placenta tissue was obtained from Chengdu Women’s and Children’s Central Hospital from April 2021 to July 2022 in Chengdu, China. The Ethics Committee of the Chengdu Women’s and Children’s Central Hospital approved the study documents and placenta collection (Permission Number: 2022(49)-2).

The inclusion criteria of ICP were as follows: 1) new-onset pruritus and elevated levels of TBA, TBA level  $> 10$  but  $< 40$   $\mu\text{mol/l}$  were categorized as mild, whereas the TBA level  $\geq 40$   $\mu\text{mol/l}$  were categorized as severe; 2) age between 18 and 35 years; 3) singleton pregnancy; 4) providing informed consent. In this study, 30 severe ICP patients (ICP-S group), 30 mild ICP patients (ICP-M group) and 30 normal pregnant women (control group) who delivered via cesarean section were recruited from the Chengdu Women’s and Children’s Central Hospital. Patients who had received infertility treatment (such as in vitro fertilization or intrauterine insemination), serious illnesses before and during pregnancy (such as chronic liver and gall bladder diseases, skin disease, hypertension, preeclampsia, diabetes, hematological diseases, kidney, and nervous system disease), and infectious diseases (such as viral hepatitis, syphilis, or acquired immune deficiency syndrome) were excluded. The villous tissue of maternal placental samples ( $3 \times 3 \times 3$  cm) was obtained immediately after delivery. The samples were flash-frozen in liquid nitrogen and stored at  $-80$  for lipidomics analysis.

### Sample preparation

Lipids were extracted as follows: 300 $\mu\text{L}$  of methanol: water (1/1, vol/vol) were added to each placental sample (30mg), and 20 $\mu\text{L}$  of LysoPC-17:0 (0.1 mg/mL, dissolved in methanol) was added as an internal standard to reflect the repeatability of the extraction, then placed into 2 steel balls and grind with a grinder (60Hz, 2min). Subsequently, 300 $\mu\text{L}$  of chloroform was added to each sample and the whole samples were extracted by ultrasonic for 10 min in an ice-water bath, stored at  $-20$  °C for 20 min. And then centrifuged at 4°C (13,000 rpm) for 10 min before decanting 200 $\mu\text{L}$  of supernatant to sample vials. 300 $\mu\text{L}$  chloroform: methanol (2/1, vol/vol, containing 0.1mM BHT) was added into the residue samples, samples vortexed for 30 s, extracted by ultrasonic for 10 min in ice-water bath, then placed at  $-20$ °C for 20 min and then centrifuged at 4°C (13,000 rpm) for 10 min prior to decanting of supernatant to sample vials. Combined two supernatants

and mixed well. Then the mixed supernatant (400 $\mu$ L) was dried under a nitrogen stream and re-dissolved in 300  $\mu$ L of isopropanol: methanol (1/1, vol/vol), vortexed for 30 s and extracted by ultrasonic for 3 min in ice-water bath, and then filtered through a 0.22  $\mu$ m organic phase pinhole filter for subsequent analysis. QC samples were prepared by mixing aliquot of all samples to be a pooled sample.

### Untargeted lipidomics analysis

LC-MS/MS analyses were performed using a Dionex Ultimate 3000 RS UHPLC fitted with Q-Exactive quadrupole-Orbitrap mass spectrometer equipped with heated electrospray ionization (ESI) source (Thermo Fisher Scientific, Waltham, MA, USA). An ACQUITY UPLC BEH C18 column (1.7  $\mu$ m, 2.1  $\times$  100 mm) was employed in both positive and negative modes. The binary gradient elution system consisted of (A) acetonitrile:water (60:40, v:v, containing 10mmol/L ammonium formate) and (B) acetonitrile: isopropanol(10:90, v:v, containing 10mmol/L ammonium formate) and separation was achieved using the following gradient:0 min, 5% B; 0.5 min, 5% B; 2 min, 43% B; 32.1 min, 52% B; 8.5 min, 53% B; 8.6 min,75% B;114 min, 90% B, 14.5in, 100% B, 15.5min, 100% B, 15.7min, 5% B and 18min, 5%B. The flow rate was 0.4 mL/min and the column temperature was 60°C. All the samples were kept at 4 °C during the analysis. The injection volume was 5  $\mu$ L. The mass spectrometer was operated in both positive ESI+ mode and negative ESI- mode. The QCs were injected at regular intervals throughout the analytical run to provide a set of data from which repeatability can be assessed.

### Data preprocessing and statistical analysis

The original Q Exactive LC-MS/MS data in raw format were processed by the software Lipid Search for MSn and the exact mass-to-charge ratio ( $m/z$ ) of parent ions. The molecular structure of lipids and the additive mode of its positive and negative ions were identified according to the parent ions and multi-stage mass spectrometry data of each sample. The results were aligned according to a certain retention time range and combined into a single report to sort out the original data matrix. In each sample, all peak signals were normalized (that is, the signal intensity of each peak is converted to the relative intensity in the spectrum, and then multiplied by 10000). The extracted data were then further processed by removing any peaks with a missing value (ion intensity = 0) in more than 50% in groups and by replacing the zero value by half of the minimum value. A data matrix was combined from the positive and negative ion data. The matrix was imported in R to carry out Principle Component Analysis (PCA) to observe the overall distribution among the samples and the stability of the whole analysis process. Orthogonal Partial Least-Squares-Discriminant Analysis (OPLS-DA) and Partial Least-Squares-Discriminant Analysis (PLS-DA) were utilized to distinguish the metabolites that differ between groups. To prevent overfitting, 7-fold cross-validation and 200 Response Permutation Testing (RPT) were used to evaluate the quality of the model.

Variable Importance of Projection (VIP) values obtained from the OPLS-DA model was used to rank the overall contribution of each variable to group discrimination. The Kyoto Encyclopedia of Genes and Genomes (KEGG) pathway database was used to analyze metabolic pathway enrichment. A weighted metabolite co-expression network was built with R package<sup>24</sup>. The co-expression module is a collection of metabolites with high topological overlap similarity. Pearson correlation analysis was used to calculate the correlation between the modules and the clinical traits to identify significant clinical modules,  $P < 0.05$  was considered as modules with significant difference. We also constructed a diagnostic model through receiver operating characteristic (ROC) curves and multiple logistic regression was used to merge multiple indicators. The statistical graphs were generated by GraphPad Prism 9 software, and a two-tailed Student's T-test was used for statistical analysis. All data are presented as the means  $\pm$  standard errors of the means (SEM). The lipids with a VIP  $\geq 1.0$  and  $P < 0.05$  were considered as significantly changed.

## Results

### 3.1 Clinical characteristics of women with ICP and normal pregnant women

Table 1 depicts the clinical characteristics of ICP and normal pregnant women. There was no significant difference in maternal age, body mass index (BMI), gravity number, parity number and placenta weight

between ICP and normal pregnant group ( $p < 0.05$ ), the gestational age at delivery was lower in both mild ICP and severe ICP group. The levels of TBA, alanine aminotransferase (ALT), and aspartate aminotransferase (AST) were significantly higher in both mild and severe ICP group compared with normal pregnancy. In addition, ICP patients had significantly lower fetal birth weight compared with healthy controls.

### 3.2 The lipid profiles of placenta collected from ICP patients

The collected placenta samples were used for lipidomic analysis through UHPLC-Q Exactive MS as described in the method section. We separately analyzed the lipid profiles between the 30 women with mild ICP or severe ICP and 30 women with normal pregnancies. To distinguish the overall differences in lipid metabolite profiles between groups, we conducted multivariate statistical modeling by using OPLS-DA. The score scatter plot of the OPLS-DA model indicated that the difference between the normal group and the mild or severe ICP group was obvious (Fig 1A and Fig 2A), the samples from the ICP-M/ICP-S group and control groups were separated along the x-axis. Permutation test was used to confirm the accuracy of the model. All Q2 values (green) on the left were lower than the original value on the right, and the regression line of Q2 values intersects the vertical axis (left) below zero, which indicates high effectiveness and good prediction ability of the OPLS-DA model (Fig 1B and Fig 2B).

A total of 61 lipids (VIP  $> 1$  and  $P < 0.05$ ) were found to be significantly different between mild ICP and control groups, which included 27 downregulated and 34 upregulated lipids in the ICP-M group. The expression levels of the 61 differential lipids were used to draw a volcano plot (Fig 1C), the blue dots represent remarkably downregulated lipids, while the red dots represent significantly upregulated lipids. The relative contents of the top 50 differentially expressed lipids were observed through a hierarchical cluster heatmap (Fig 1D). All of the differentially expressed lipids can be classified into 16 categories, including: 15 PE species, 10 PC species, seven PS species, 12 SM species, three TG species, two FA species, two dMePE species, and one OAHFA, MGDG, Cer, GM3, phSM, LPE, ChE, PG, PI species. Detailed information about these differential lipids is shown in Data S1.

We also obtained 88 differential lipids between severe ICP and the control group according to the conditions of VIP  $> 1$  and  $P < 0.05$ . A total of 46 lipids exhibited increased levels, and 42 exhibited decreased levels in the ICP-S group, and the detailed information between these two groups was shown in Data S2. The heatmap and volcano plots were conducted to display differences in lipid metabolites between the two groups (Fig 2C and Fig 2D). All the 88 differential lipids can be classified into 17 categories, including 20 PC species, 19 PE species, 15 PS species, 13 SM species, seven TG species, two dMePE species, two So species, and one OAHFA, MGDG, Cer, GM3, phSM, LPE, ChE, PG, PI, FA species, respectively.

### 3.3 Critical lipids screening through Venn Diagram and Pathway analysis

We identified 44 lipids differentially expressed both in the mild and severe ICP group compared with the control group (Fig 3A). Detailed information regarding the 44 differential lipids was shown in Table 2. To screen critical lipids that are associated with ICP, we combined the previously published ICP plasma lipidomics data for further analysis<sup>23</sup>. In the previously reported data, Sun et al revealed differentially expressed plasma lipids in ICP patients, and we identified three differential lipids co-expressed both in ICP placenta and ICP plasma (Fig 3A). These three lipids are SM (d42:1), SM (d18:1/24:1) and PC (17:0/18:2), and their expression level in the ICP placenta is significantly altered (Fig 3C). Based on the identified 44 differential lipids, we conducted a pathway analysis to reveal possible metabolic pathways involved in ICP onset. The results of the pathway analysis show that the significantly altered lipids were enriched in autophagy regulation, glycerophospholipid metabolism and GPI-anchor biosynthesis (Fig 3B). It was reported autophagy is closely related to ICP pathogenesis<sup>14, 25, 26</sup>, we further analyzed the individual autophagy pathways and found 5 PE lipids are closely in correlation with autophagy (Fig S1), including PE (16:0/18:1), PE (16:0/20:2), PE (18:1/20:3), PE (18:1/20:4), exhibited increased level in ICP placenta, while PE (18:0/22:4) exhibited decreased expression level (Fig 3C), indicate these lipids may play a pivotal role in the occurrence and development of ICP.

### 3.4 Critical lipid Co-expression network modules closely correlated with ICP

To clarify the relationships between lipids profile and the clinical characteristics of our study population, we next constructed Weighted Gene Co-expression Network Analysis (WGCNA) to identify clusters or modules that have similar expression patterns. In this analysis, we obtained 14 modules and the result showed that most lipids were clustered in turquoise, yellow and pink modules (Fig S2). Among the 14 modules, the pink module and purple module showed a significant positive correlation with TBA, ALT and AST levels, whereas the salmon module negatively correlated with TBA, ALT and AST levels (Fig 4A). A total of 30 lipids were included in these three modules, and we identified 11 differentially co-expressed lipids overlapped with the dysregulated lipids in both mild and severe ICP group (Fig S3A). Next, the CytoScape was used to screen hub lipids in pink, purple and salmon module based on the MCC algorithm. The top 4 lipids in the MCC algorithm were identified as hub lipids. As shown in Fig 4B, we identified PE (18:0p/20:1), dMePE (20:1p/16:0), PE (16:0p/22:1) and PE (38:2e) as hub lipids in the pink module. Among these four hub lipids, the expression level of PE (18:0p/20:1), dMePE (20:1p/16:0) and PE (16:0p/22:1) was significantly elevated in the mild and severe ICP group (Fig 4C). The network diagram also depicts the hub lipids in purple and salmon module (Fig S3B and Fig S3C).

### 3.5 Diagnostic utility of ICP placenta differential lipids

We constructed ROC curves and calculated AUCs to evaluate the probability of these lipids being diagnosed with ICP. As shown in Fig 5A-C, the AUCs of SM (d42:1), SM (d18:1/24:1) and PC (17:0/18:2) were 0.718, 0.768 and 0.748, respectively. And the AUCs of PE (18:0p/20:1), dMePE (20:1p/16:0) and PE (16:0p/22:1) were 0.735, 0.723 and 0.764 (Fig 5D-F). We also evaluate the diagnostic utility of 5 lipids identified from autophagy pathway analysis, results showed the AUCs of PE (16:0/18:1), PE (16:0/20:2), PE (18:0/22:4), PE (18:1/20:3) and PE (18:1/20:4) were 0.682, 0.649, 0.665, 0.659 and 0.657, respectively (Fig S4). Using multiple logistic regression analysis, we found that a good diagnostic model for ICP could be constructed by combining these lipids. Analysis results of combined biomarker data yielded an AUC of 0.904 for PE (16:0/20:2), SM (d42:1) and PC (17:0/18:2) (Fig 5G). The AUCs even reach 0.933 when combining PE (16:0/20:2), SM (d42:1), PC (17:0/18:2) and PE (16:0p/22:1) (Fig 5H). Therefore, the combination of these lipids could be reliable, and a novel biomarker in predicting the risk of ICP.

## Discussion

Intrahepatic cholestasis of pregnancy is associated with increased risk of perinatal mortality and morbidity, however, the pathogenesis of ICP is still unclear. There is no effective treatment for ICP currently, once ICP is diagnosed, the only effective way to prevent adverse pregnancy outcomes is delivery<sup>27</sup>. As an emerging field that branches from metabolomics, more and more lipidomics proved that lipids have multiple functions and are involved in many biological processes. Previous studies suggested that placental lipid profiles, for example, LDL cholesterol and sphingolipids differed between normal pregnant women and ICP patients<sup>23, 28</sup>. Given that lipid metabolic dysregulation potentially plays a role in pregnancy, a better understanding of lipid metabolism could have significant clinical implications for the diagnosis and treatment of ICP.

In this study, we found ICP placenta has a significantly different lipid profile from normal pregnancy. A total of 61 lipids were found to be dysregulated in mild ICP placenta, and the differentially expressed lipids mainly include PE, PC, PS and SM species. We also identified 88 differential lipids between severe ICP placenta and normal pregnancy, and these lipids mainly include PE, PC, PS, SM and TG species. Among these lipids, we identified 44 lipids differentially expressed both in mild and severe ICP group compared with the control group, mainly of them were SM, PE, PC and PS species. Moreover, pathway analysis of the placentas of patients with ICP identified autophagy regulation, glycerophospholipid metabolism and GPI-anchor biosynthesis, suggesting these pathways might be related to the pathogenesis of ICP.

Autophagy is an evolutionally conserved process that targets cytoplasmic components such as organelles, protein aggregates or proteins for degradation into lysosomes to maintain cellular homeostasis under environmental stress<sup>29, 30</sup>. Autophagy plays a pivotal role in implantation, embryogenesis and maintenance of pregnancy<sup>31</sup>. A previous study demonstrated the expression of LC3-II is elevated in ICP human placenta and placentas of ICP rats, indicating autophagy is closely related to ICP<sup>25</sup>. Zhang et al used TCA-treated term

placental villous for proteomic analysis, their results revealed protein expression difference in ICP mainly related to autophagy and cell metabolism<sup>32</sup>. Consistent with their result, Fang et al analyzed 10 ICP and 10 normal placental tissue through quantitative proteomics and their results showed the differentially expressed proteins mainly participated in autophagy, autophagosome formation and metabolism<sup>33</sup>. All of these indicate a close correlation between ICP and autophagy. In our lipidomic analysis, we also found the differentially expressed lipids mainly enriched in the autophagy pathway, and PE (16:0/18:1), PE (16:0/20:2), PE (18:1/20:3), PE (18:1/20:4) and PE (18:0/22:4) participated in this process. Phosphatidylethanolamine (PE) is the second most abundant phospholipid in the membranes of all mammalian cells<sup>34, 35</sup>. As a fundamental component of biological membranes, PE is essential for many cellular functions and the dysregulation of PE metabolism has been implicated in many diseases, such as nonalcoholic liver disease, atherosclerosis and obesity<sup>36, 37</sup>. In addition, PE is essential for the formation of LC3-II in the autophagolysosomal bilayer membrane. During autophagy, a cytosolic form of LC3-I is conjugated to phosphatidylethanolamine to form LC3- phosphatidylethanolamine conjugate, that is LC3-II, which is recruited to autophagosomal membranes. The autophagosomal marker LC3-II could reflect autophagic activity, and detecting LC3-II has become a reliable method for monitoring autophagy and autophagy-related processes<sup>38</sup>. Therefore, excessive accumulation of PE (16:0/18:1), PE (16:0/20:2), PE (18:1/20:3) and PE (18:1/20:4) in ICP placenta may lead to the formation of LC3-II and eventually the activation of autophagy pathway, which has been confirmed to be involved in the pathogenesis and development of ICP.

Through combined analysis with previous studies, we also identified SM (d42:1), SM (d18:1/24:1) and PC (17:0/18:2) are differentially expressed both in ICP placenta and plasma samples. And their good diagnostic utility was also accessed through the construction of ROC curves. Two of these three lipids were sphingolipids. The sphingolipid metabolic pathway produces bioactive metabolites like sphingosine 1-phosphate (S1P), ceramide and sphingosine, they can participate in various biological processes such as cell survival, growth, vascular integrity and inflammation. Sphingolipids have been proven to be related to pregnancy-associated complications such as preeclampsia, recurrent pregnancy loss and intrauterine growth restriction<sup>39-41</sup>. A previous study reported the median values of C16-Cer and C18-Cer were significantly increased in the plasma of ICP patients, and after treatment with UDCA for a week, the concentration of C16-Cer and C18-Cer decreased considerably<sup>42</sup>. Consistent with their finding, Sun et al also reported ICP is associated with disordered sphingolipid homeostasis<sup>23</sup>. Collectively, this evidence proved that sphingolipids may act as new diagnostic targets for ICP.

There are still several limitations in our study. First, further animal and cellular experiments are needed to elucidate the specific mechanisms of lipid changes. Second, many studies on lipidomics and ICP have been conducted with a small number of patients, which limits the generalizability of the findings. Larger studies are needed to confirm the role of lipids in ICP. Finally, the diagnosis of ICP is currently based on clinical symptoms and biochemical tests. However, there is a lack of standardized criteria for the diagnosis of ICP, which can lead to variability in patient selection and make it challenging to compare results across studies.

In conclusion, we used UHPLC to characterize the placental lipidomics profiling for women complicated with ICP. Our results confirmed there were significant changes in lipid profile in the mid and severe ICP placenta, the metabolic pathway was primarily associated with autophagy and glycerophospholipid metabolism. And ICP placenta is associated with dysregulation of sphingolipid homeostasis. Our research highlighted some important mechanisms involved in the onset of ICP and might provide new insight into the treatment and diagnosis of ICP.

## Abbreviations

ICP Intrahepatic cholestasis of pregnancy

TBAs total bile acids

UDCA ursodeoxycholic acid

EASL The European Association for the Study of the Liver

SMFM the Society for Maternal-Fetal Medicine

CA cholic acid

CDCA chenodeoxycholic acid

ALT alanine aminotransferase

AST aspartate aminotransferase

LDL Low-density lipoprotein TC Total cholesterol TG Triglyceride UHPLC-Q Exactive MS Ultrahigh-performance liquid chromatography plus Q-Exactive mass spectrometry PC Phosphocholine

LPC Lysophosphocholine IDL Intermediate-density lipoprotein LC-MS Liquid chromatography coupled with MS SM Sphingomyelin CE Electrophoresis PE Phosphatidylethanolamine PS Phosphatidylserine Cer Ceramide LPE Lysophosphatidylethanolamine CE Cholesteryl esters DAG Diacylglycerol ESI Electrospray ionization PA Phosphatidic acid PCA Principal component analysis OPLS-DA Orthogonal partial least squares-discriminant analysis PLS-DA Partial least squares-discriminant analysis VIP Variable importance of projection KEGG Kyoto Encyclopedia of Genes and Genomes

### **Ethics approval and consent to participate**

Not applicable

### **Consent for publication**

Not applicable

### **Availability of data and materials**

Not applicable

### **Competing interests**

The authors declare that they have no competing interests.

### **Funding**

This work was supported by grants from the National Natural Science Foundation of China, Grant/Award Number: 82201864; the Project of Chengdu Women and Children's Central Hospital, Grant/Award Number: YC2022003 / 2022JC01; the Key Research and Development Project of Sichuan Province, Grant/Award Number: 2022YFS0227 / 2023NSFSC1610; and the China Postdoctoral Science Foundation, Grant/Award Number: 2022M710617.

### **Authors' contributions**

Liling Xiong and Mi Tang processed the data and wrote the manuscript. Hong Liu, Ying Jin, and Xiu Yang collected the clinical data and placenta samples. Jianghui Cai and Cheng Huang participated in the production of tables. Shasha Xing and Xiao Yang supervised the whole study.

### **Acknowledgments**

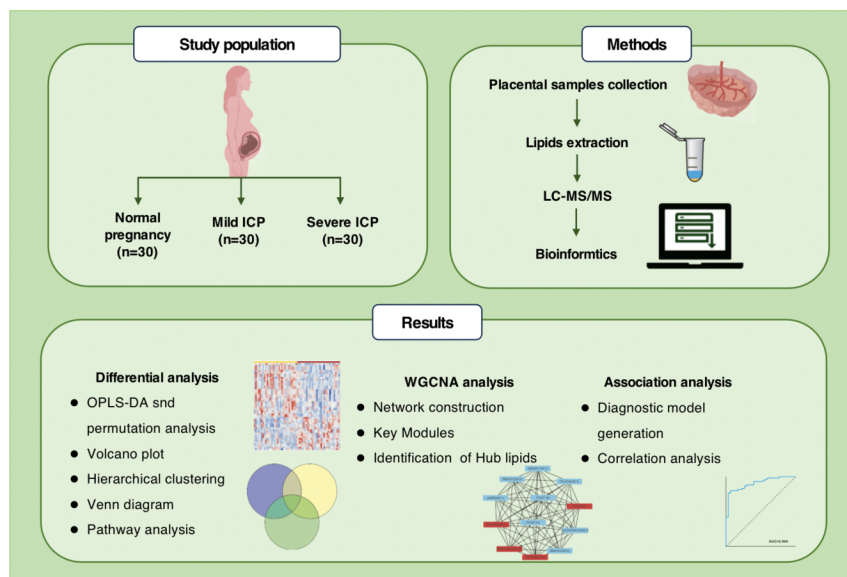
Not applicable

### **Reference:**

1. Abdelhafez, M.M.A., et al., Intrahepatic cholestasis of pregnancy: from an obstetrician point of view. *J Obstet Gynaecol*, 2022: p. 1-8.
2. Bicocca, M.J., J.D. Sperling, and S.P. Chauhan, Intrahepatic cholestasis of pregnancy: Review of six national and regional guidelines. *Eur J Obstet Gynecol Reprod Biol*, 2018. 231: p. 180-187.

3. Glantz, A., H.U. Marschall, and L.A. Mattsson, Intrahepatic cholestasis of pregnancy: Relationships between bile acid levels and fetal complication rates. *Hepatology*, 2004. 40(2): p. 467-74.
4. Gao, X.X., et al., Prevalence and risk factors of intrahepatic cholestasis of pregnancy in a Chinese population. *Sci Rep*, 2020. 10(1): p. 16307.
5. Chappell, L.C., et al., Ursodeoxycholic acid versus placebo in women with intrahepatic cholestasis of pregnancy (PITCHES): a randomised controlled trial. *Lancet*, 2019. 394(10201): p. 849-860.
6. Kumar, P. and A. Kulkarni, UDCA therapy in intrahepatic cholestasis of pregnancy? *J Hepatol*, 2020. 72(3): p. 586-587.
7. Lee, R.H., et al., Society for Maternal-Fetal Medicine Consult Series #53: Intrahepatic cholestasis of pregnancy: Replaces Consult #13, April 2011. *Am J Obstet Gynecol*, 2021. 224(2): p. B2-b9.
8. Geenes, V., et al., Association of severe intrahepatic cholestasis of pregnancy with adverse pregnancy outcomes: a prospective population-based case-control study. *Hepatology*, 2014. 59(4): p. 1482-91.
9. Kawakita, T., et al., Predictors of adverse neonatal outcomes in intrahepatic cholestasis of pregnancy. *Am J Obstet Gynecol*, 2015. 213(4): p. 570.e1-8.
10. Brites, D., et al., Correction of maternal serum bile acid profile during ursodeoxycholic acid therapy in cholestasis of pregnancy. *J Hepatol*, 1998. 28(1): p. 91-8.
11. Kondrackiene, J. and L. Kupcinskas, Intrahepatic cholestasis of pregnancy-current achievements and unsolved problems. *World J Gastroenterol*, 2008. 14(38): p. 5781-8.
12. Ozkan, S., et al., Review of a challenging clinical issue: Intrahepatic cholestasis of pregnancy. *World J Gastroenterol*, 2015. 21(23): p. 7134-41.
13. Wei, W. and Y.Y. Hu, Expression of hypoxia-regulated genes and glycometabolic genes in placenta from patients with intrahepatic cholestasis of pregnancy. *Placenta*, 2014. 35(9): p. 732-6.
14. Shan, D., R. Dong, and Y. Hu, Current understanding of autophagy in intrahepatic cholestasis of pregnancy. *Placenta*, 2021. 115: p. 53-59.
15. Han, X. and R.W. Gross, The foundations and development of lipidomics. *J Lipid Res*, 2022. 63(2): p. 100164.
16. Wang, Y., et al., Plasma lipidomics in early pregnancy and risk of gestational diabetes mellitus: a prospective nested case-control study in Chinese women. *Am J Clin Nutr*, 2021. 114(5): p. 1763-1773.
17. Morillon, A.C., et al., Association between phospholipid metabolism in plasma and spontaneous preterm birth: a discovery lipidomic analysis in the cork pregnancy cohort. *Metabolomics*, 2020. 16(2): p. 19.
18. Zhang, L., et al., Integrated Metabolomic and Lipidomic Analysis in the Placenta of Preeclampsia. *Front Physiol*, 2022. 13: p. 807583.
19. Li, Y., et al., Targeted metabolomics of sulfated bile acids in urine for the diagnosis and grading of intrahepatic cholestasis of pregnancy. *Genes Dis*, 2018. 5(4): p. 358-366.
20. Cui, Y., et al., Diagnostic and therapeutic profiles of serum bile acids in women with intrahepatic cholestasis of pregnancy—a pseudo-targeted metabolomics study. *Clin Chim Acta*, 2018. 483: p. 135-141.
21. Hao, Z.M., et al., Lipoprotein lipase and lipid profiles in plasma and placenta from normal pregnancies compared with patients with intrahepatic cholestasis of pregnancy. *Eur J Obstet Gynecol Reprod Biol*, 2016. 203: p. 279-85.
22. Fiorucci, S., et al., Bile-acid-activated receptors: targeting TGR5 and farnesoid-X-receptor in lipid and glucose disorders. *Trends Pharmacol Sci*, 2009. 30(11): p. 570-80.

23. Sun, X., et al., Untargeted lipidomics analysis in women with intrahepatic cholestasis of pregnancy: a cross-sectional study. *BJOG*, 2022. 129(6): p. 880-888.
24. Langfelder, P. and S. Horvath, WGCNA: an R package for weighted correlation network analysis. *BMC Bioinformatics*, 2008. 9: p. 559.
25. Hu, J., et al., Linc02527 promoted autophagy in Intrahepatic cholestasis of pregnancy. *Cell Death Dis*, 2018. 9(10): p. 979.
26. Dong, R., et al., Elevated GABRP expression is correlated to the excessive autophagy in intrahepatic cholestasis of pregnancy. *Heliyon*, 2023. 9(2): p. e13221.
27. Mathur, D., et al., Intrahepatic cholestasis of pregnancy: dilemma in diagnosis and management. *J Matern Fetal Neonatal Med*, 2022. 35(25): p. 8975-8981.
28. Dann, A.T., et al., Plasma lipid profiles of women with intrahepatic cholestasis of pregnancy. *Obstet Gynecol*, 2006. 107(1): p. 106-14.
29. Klionsky, D.J., et al., Autophagy in major human diseases. *Embo j*, 2021. 40(19): p. e108863.
30. Cao, W., et al., An overview of autophagy: Mechanism, regulation and research progress. *Bull Cancer*, 2021. 108(3): p. 304-322.
31. Nakashima, A., et al., Current Understanding of Autophagy in Pregnancy. *Int J Mol Sci*, 2019. 20(9).
32. Zhang, T., et al., Comparative proteomics analysis of placenta from pregnant women with intrahepatic cholestasis of pregnancy. *PLoS One*, 2013. 8(12): p. e83281.
33. Fang, D., et al., Comprehensive Analysis of Quantitative Proteomics With DIA Mass Spectrometry and ceRNA Network in Intrahepatic Cholestasis of Pregnancy. *Front Cell Dev Biol*, 2022. 10: p. 854425.
34. van der Veen, J.N., et al., The critical role of phosphatidylcholine and phosphatidylethanolamine metabolism in health and disease. *Biochim Biophys Acta Biomembr*, 2017. 1859(9 Pt B): p. 1558-1572.
35. Vance, J.E., Phosphatidylserine and phosphatidylethanolamine in mammalian cells: two metabolically related aminophospholipids. *J Lipid Res*, 2008. 49(7): p. 1377-87.
36. Calzada, E., O. Onguka, and S.M. Claypool, Phosphatidylethanolamine Metabolism in Health and Disease. *Int Rev Cell Mol Biol*, 2016. 321: p. 29-88.
37. Fu, S., et al., Aberrant lipid metabolism disrupts calcium homeostasis causing liver endoplasmic reticulum stress in obesity. *Nature*, 2011. 473(7348): p. 528-31.
38. Runwal, G., et al., LC3-positive structures are prominent in autophagy-deficient cells. *Sci Rep*, 2019. 9(1): p. 10147.
39. Del Gaudio, I., et al., Sphingolipid Signature of Human Feto-Placental Vasculature in Preeclampsia. *Int J Mol Sci*, 2020. 21(3).
40. Wang, L.L., et al., The metabolic landscape of decidua in recurrent pregnancy loss using a global metabolomics approach. *Placenta*, 2021. 112: p. 45-53.
41. Chauvin, S., et al., Aberrant TGF $\beta$  Signalling Contributes to Dysregulation of Sphingolipid Metabolism in Intrauterine Growth Restriction. *J Clin Endocrinol Metab*, 2015. 100(7): p. E986-96.
42. Mikucka-Niczyporuk, A., et al., Role of sphingolipids in the pathogenesis of intrahepatic cholestasis. *Prostaglandins Other Lipid Mediat*, 2020. 147: p. 106399.



**Graphical abstract** . Overview of study design. Untargeted lipidomics workflow and data processing.

### Figure legend

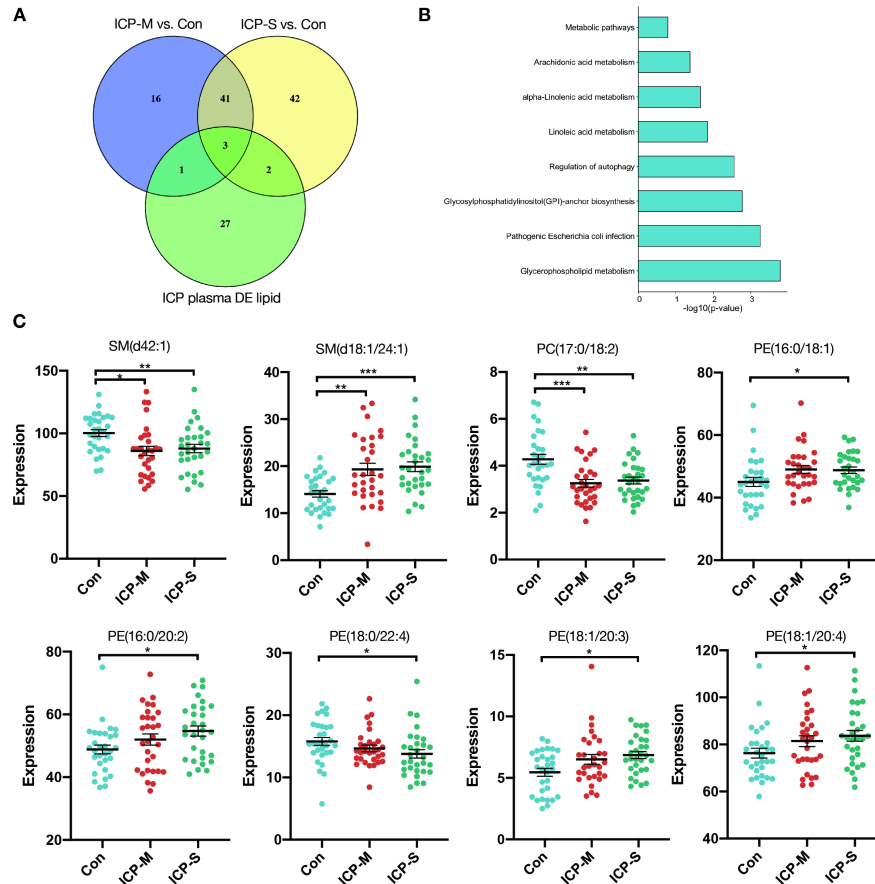
**Fig 1.** LC-MS/MS lipidomics analysis between the mild ICP and control group. **(A)** The score plot of the supervised orthogonal partial least squares discriminant analysis (OPLS-DA) of mild ICP (yellow) and control (red) group. **(B)** Permutation analysis. R2x (cum) and R2y (cum) represent the cumulative interpretation rate of the model in the x-axis and y-axis directions, respectively. Cum represents the accumulation of several principal components. Q2 (cum) represents the cumulative prediction rate of the model. **(C)** Volcano plots of the levels of differentially expressed lipids. Red indicates increased levels, blue indicates decreased levels, and gray indicates no statistical significance. **(D)** Hierarchical clustering of each sample data set showing the differentially expressed lipids.

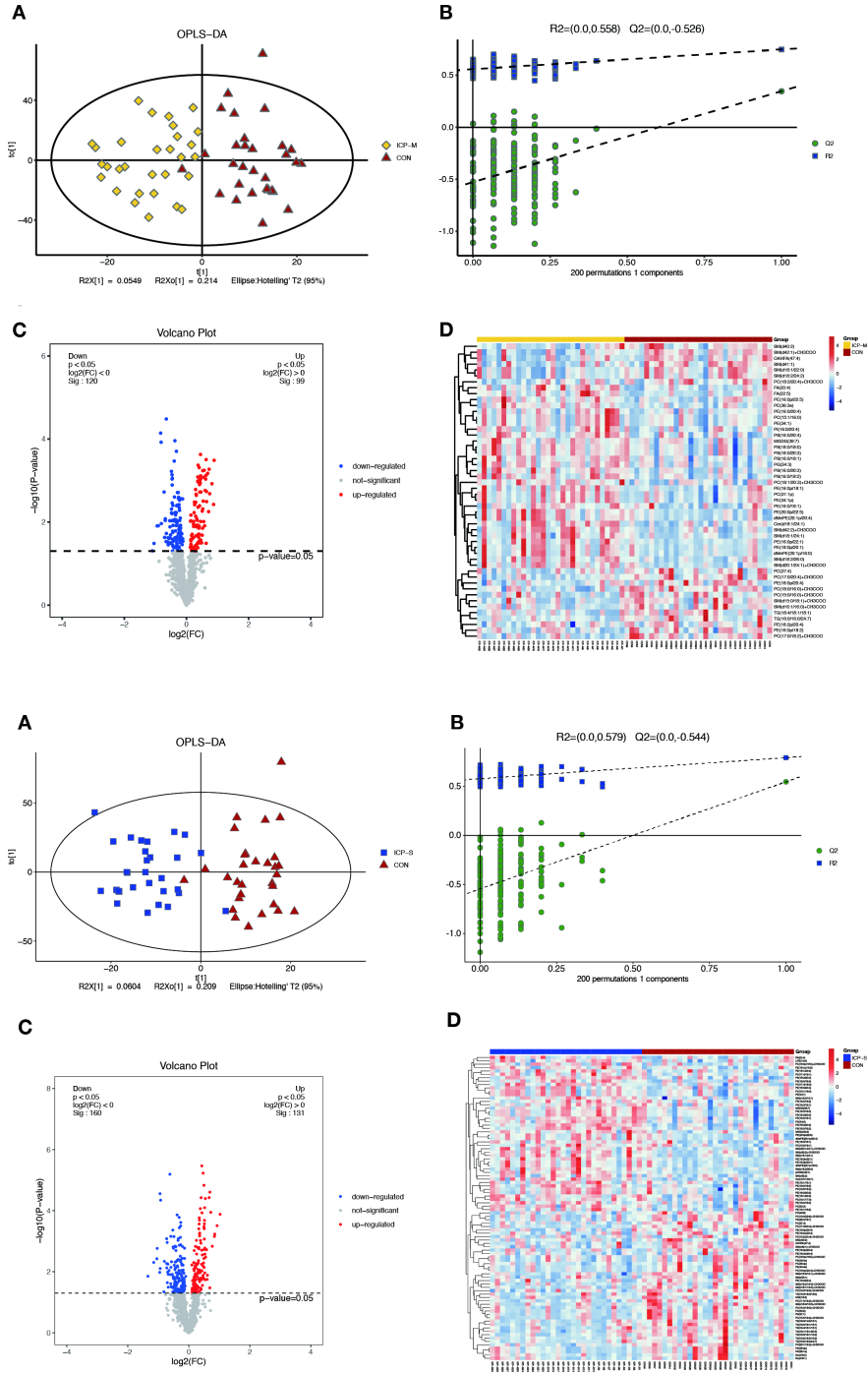
**Fig 2.** LC-MS/MS lipidomics analysis between the severe ICP and control group. **(A)** The score plot of the OPLS-DA of severe ICP (blue) and control (red) group. **(B)** Permutation analysis. R2x (cum) and R2y (cum) represent the cumulative interpretation rate of the model in the x-axis and y-axis directions, respectively. Cum represents the accumulation of several principal components. Q2 (cum) represents the cumulative prediction rate of the model. **(C)** Volcano plots of the levels of differentially expressed lipids. Red indicates increased levels, blue indicates decreased levels, and gray indicates no statistical significance. **(D)** Hierarchical clustering of each sample data set showing the differentially expressed lipids.

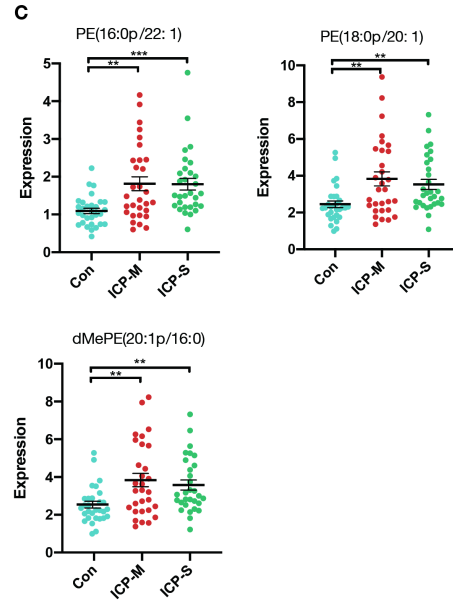
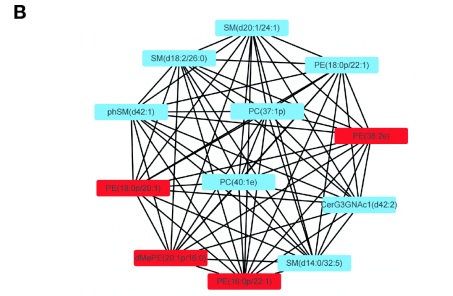
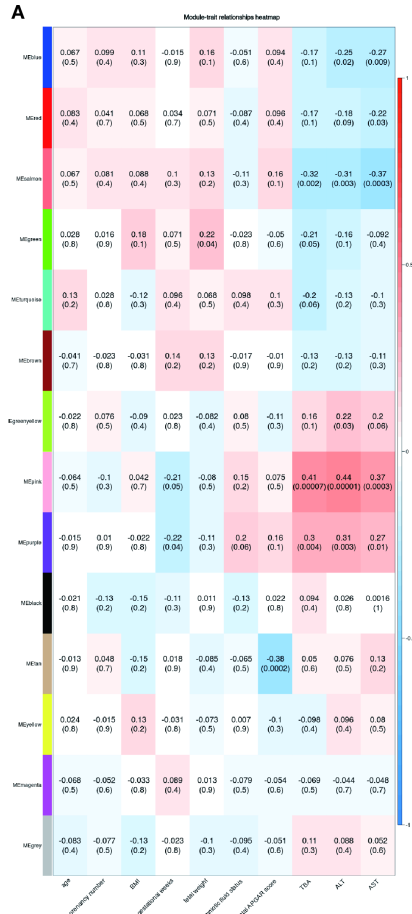
**Fig 3.** Differentially expressed lipids in the mild and severe group and the pathway analysis. **(A)** Venn diagram of the differentially expressed lipids in ICP placenta and ICP plasma. **(B)** Pathway analysis of 44 differentially altered lipids. **(C)** Intensity of differential lipids expression in the control (blue), mild ICP (red) and severe ICP (green). Data are presented as the means  $\pm$  SEMs. Significance was assessed using a two-tailed Student's t-test. \* $P$   $\leq$  0.05, \*\* $P$   $\leq$  0.01, \*\*\* $P$   $\leq$  0.0001 vs. the control group.

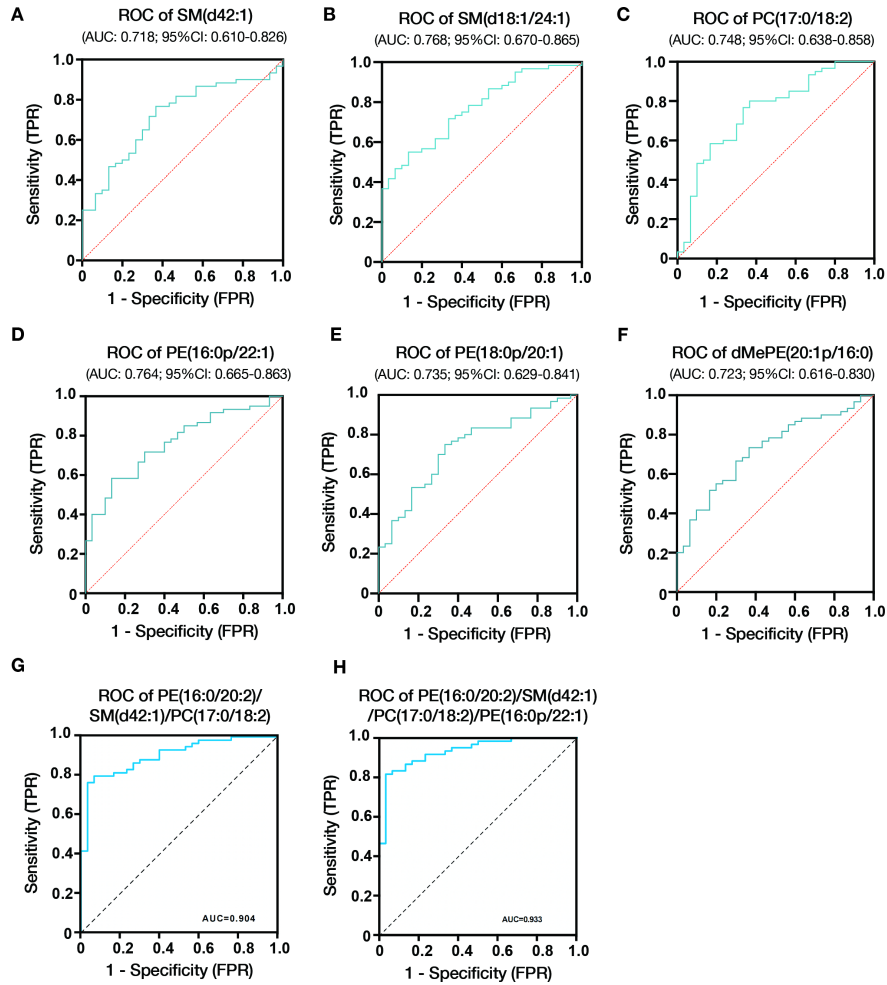
**Fig 4.** WGCNA analysis and identification of lipids associated with the clinical traits of ICP. **(A)** Pearson correlation analysis of the lipids module and clinical traits, the red color indicates a positive correlation and blue indicates negative correlation. The depth of the color indicates the strength of the correlation. **(B)** Hub lipids in pink module was screened out by CytoScape. **(C)** Intensity of differential hub lipids expression in the pink module. Data are presented as the means  $\pm$  SEMs. Significance was assessed using a two-tailed Student's t-test. \*\* $P$   $\leq$  0.01, \*\*\* $P$   $\leq$  0.0001 vs. the control group.

**Fig 5.** Diagnostic utility of differential lipids in placenta from ICP pregnant women. **(A)** ROC analysis of SM (d42:1). **(B)** ROC analysis of SM (d18:1/24:1). **(C)** ROC analysis of PC (17:0/18:2). **(D)** ROC analysis of PE (16:0p/22:1). **(E)** ROC analysis of PE (18:0p/20:1). **(F)** ROC analysis of dMePE (20:1p/16:0). Multiple logistic regression analysis showed the combined ROC analysis of PE (16:0/20:2)/SM (d42:1)/PC (17:0/18:2) **(G)** and PE (16:0/20:2)/SM (d42:1)/PC (17:0/18:2)/PE (16:0p/22:1) **(H)**. AUC, area under the curve; CI, confidence interval; ROC, receiver operating characteristic.









### Hosted file

Table1 Clinical characteristics of the participants.docx available at <https://authorea.com/users/639534/articles/654800-lc-ms-ms-based-untargeted-lipidomics-uncovers-lipid-signatures-of-the-human-placenta-from-intrahepatic-cholestasis-of-pregnancy>

### Hosted file

Table2-venn diagram lipids.docx available at <https://authorea.com/users/639534/articles/654800-lc-ms-ms-based-untargeted-lipidomics-uncovers-lipid-signatures-of-the-human-placenta-from-intrahepatic-cholestasis-of-pregnancy>